# Decoupling strategy-enabled radical generality via an asymmetric $S_H2$ path

Li-Wen Fan[1,2,5], Jun-Bin Tang[1,2,5], Li-Lei Wang[1,2,5], Ji-Ren Liu[1,2,4,5], Zhong-Liang Li[3], Yu-Shuai Zhang[3], Dai-Lei Yuan[3], Li Qin[1,2], Cheng Luan[3], Qiang-Shuai Gu[3] ✉, Xin Hong[4] ✉, Zhe Dong[1,2] ✉ & Xin-Yuan Liu[1,2] ✉

[1]Shenzhen Grubbs Institute, Department of Chemistry, and Guangming Advanced Research Institute, Southern University of Science and Technology, Shenzhen, China.

[2]Shenzhen Key Laboratory of Cross-Coupling Reactions, Southern University of Science and Technology, Shenzhen, China.

[3]Academy for Advanced Interdisciplinary Studies and Department of Chemistry, Southern University of Science and Technology, Shenzhen, China.

[4]Center of Chemistry for Frontier Technologies, Department of Chemistry, State Key Laboratory of Clean Energy Utilization, Zhejiang University, Hangzhou, China.

[5]These authors contributed equally: Li-Wen Fan, Jun-Bin Tang, Li-Lei Wang, Ji-Ren Liu.

✉email: guqs@sustech.edu.cn; hxchem@zju.edu.cn; dongz@sustech.edu.cn; liuxy3@sustech.edu.cn

**Abstract**

Reaction generality is essential for evaluating the value and impact of a synthetic method. However, asymmetric catalysis, particularly that involving highly reactive species such as radicals, typically prioritizes enantioselectivity at the expense of generality. Selectivity and reactivity often conflict because the bond-forming step is usually also stereodetermining. If these two steps were separated, the reaction selectivity and generality issues could then be addressed independently. Herein we report a catalytic asymmetric radical coupling with great generality by merging the copper-catalyzed enantioselective S(IV) center formation and copper-mediated enantiospecific $S_H2$ radical coupling. This decoupling strategy has enabled the successful coupling of over 30 different carbon-, nitrogen-, and oxygen-based radicals having a broad range of reactivity with *N*-acyl sulfenamides, leading to diverse S-chiral compounds with exceptional enantioselectivity. Thus, it offers a holistic approach to accessing a rich portfolio of S(IV) and S(VI) chiral centers, which is anticipated to have a transformative impact on the synthesis of S-chiral compounds and benefit medicinal chemistry and other related fields. Furthermore, this decoupling strategy via $S_H2$ processes has promising potential to enable a comprehensive single-electron methodology for forging other chiral centers with heteroatoms such as phosphorous(III) and silicon(IV), and eventually also carbon atoms.

**Main Text:**

Robust organic synthetic methods have played an unparalleled role in the world of new molecule synthesis[1–3]. Developing a reaction with both a high yield and a broad scope (reaction generality) is the ultimate goal for synthetic chemists[4]. Indeed, powerful synthetic methods can even change the target that people want to make[5]. For example, due to the great generality of palladium-catalyzed C($sp^2$)–C($sp^2$) cross-coupling, arenes and heteroarenes have become the most common functional groups in the FDA-approved drugs[6–8]. On the other hand, catalytic asymmetric reactions pose an additional enantioselectivity issue (Fig. 1a)[9,10], which significantly complicates the optimization of reaction conditions[11]. In reality, the development of a catalytic asymmetric reaction with great generality (broad scopes with high selectivity; Fig. 1a, right) comparable to that of palladium-catalyzed C($sp^2$)–C($sp^2$) cross-coupling still remains a formidable challenge, particularly for those involving highly reactive species[12]. This challenge in asymmetric synthesis involves the most often trade-off between high reactivity and high stereoselectivity, which is vividly portrayed in the reactions involving highly reactive carbocation intermediates. These transformations, renowned for their excellent reactivity, frequently face significant obstacles in securing enantioselective control (Fig. 1a, left)[13]. Conversely, certain reactions, while demonstrating remarkable enantioselectivity, are constrained in their scopes (Fig. 1a, middle). In this aspect, natural enzyme-catalyzed reactions serve as a compelling testament, being meticulously evolved over millennia for only a few selected substrates[14,15]. In a parallel fashion, chemical asymmetric catalysis has historically emphasized enantioselectivity over the breadth of reaction scope. To gain a general catalytic asymmetric reaction scope, a long catalyst optimization campaign is often required even for a quite limited chemical space[16]. Recent strategies, such as multi-substrate screening, show promise in reducing the optimization efforts[10,11,17]. Nevertheless, their widespread implementation is still in its infancy.

The primary obstacle in developing a broadly applicable, catalytic asymmetric reaction with highly reactive species can be rationalized by a typical bond-coupling catalytic cycle (Fig. 1b). It is quite intuitive that the new chemical bond formation step (Fig. 1b, Step C), which generates a new stereocenter, should be the stereodetermining step for the whole catalytic cycle. Accordingly, Step A and Step B usually do not contribute to the reaction enantioselectivity. The intrinsic high reactivity of in-situ-formed species, like **B'**, most often significantly compromise the stereodiscrimination abilities of chiral catalysts. And the higher the reactivity of species **B'**, the more difficult the stereochemical control becomes. This phenomenon frequently appears in the field of catalytic asymmetric reactions involving highly reactive intermediates such as radicals[12,18].

On the contrary, if the bond formation step is not stereodetermining, the dilemma of reactivity and selectivity might be mitigated accordingly (Fig. 1c)[19–21]. As such, we hypothesized that using distinct in-cycle catalytic species to address the reactivity and selectivity issues separately could be the key to solve the generality challenge. In this ideal scenario, an earlier Step B (Fig. 1c) might determine the enantioselectivity and the bond-forming Step C (Fig. 1c) would only contribute to the reaction scope. In this way, decoupling the reactivity and selectivity issues would effectively allow synthetic chemists more flexibility to resolve both problems using a single catalyst. Therefore, this strategy of decoupling reactivity and selectivity could serve as a universal approach to improve the generality of catalytic asymmetric reactions.

To test this concept and considering the normally high reaction rate and stereospecificity of a bimolecular homolytic substitution ($S_H2$) reaction[22], we envisioned that it would be an ideal candidate for Step C. The $S_H2$ substitution is conceptually similar to an $S_N2$ (bimolecular nucleophilic substitution) reaction in nature. The attacking "nucleophile" in $S_H2$ is an open-shell species such as organic radicals and the "electrophile" being attacked breaks the leaving group bond in a homolytic way, unlike the heterolytic

manner involved in $S_N2$[23,24]. Thanks to the high reactivity of organic radicals, this process has been widely leveraged to construct diverse carbon–carbon[25], carbon–heteroatom[26,27], and heteroatom-heteroatom bonds[28]. Moreover, it has a unique advantage in the formation of hindered chemical bonds, such as those attached to a quaternary carbon center, under mild conditions[29]. However, there has been only a preliminary success in achieving the catalytic enantioselective $S_H2$ processes by enzyme catalysis[30] and biomimetic chiral metal catalysis[31,32], likely due to their commonly very low activation energies[22].

Considering all these facts, we believed that it would be better to transfer chirality instead of creating it de novo via the $S_H2$ process[33]. As such, by applying the abovementioned decoupling strategy (Fig. 1c), we expected to generate a chiral intermediate with excellent enantioselectivity in the earlier part of the catalytic cycle. The chiral information would then be transferred to the final product via an enantiospecific $S_H2$ process. We anticipated that this decoupling approach could offer both excellent enantioselectivity and wide reaction generality. Herein, we describe our efforts in developing a highly versatile catalytic asymmetric radical cross-coupling of *N*-acyl sulfenamides with exceptionally diverse electrophiles. Accordingly, the reaction readily accommodates more than 30 different C-, N-, and O-based radicals with a broad range of reactivity, thus providing convenient access to all sorts of highly enantioenriched S(IV) and S(VI) compounds. This superior reaction generality hinges on a decoupled process consisting of copper-catalyzed enantioselective S(IV) center formation and copper-sulfinimidoyl complex-mediated enantiospecific $S_H2$ radical coupling (Fig. 1d).

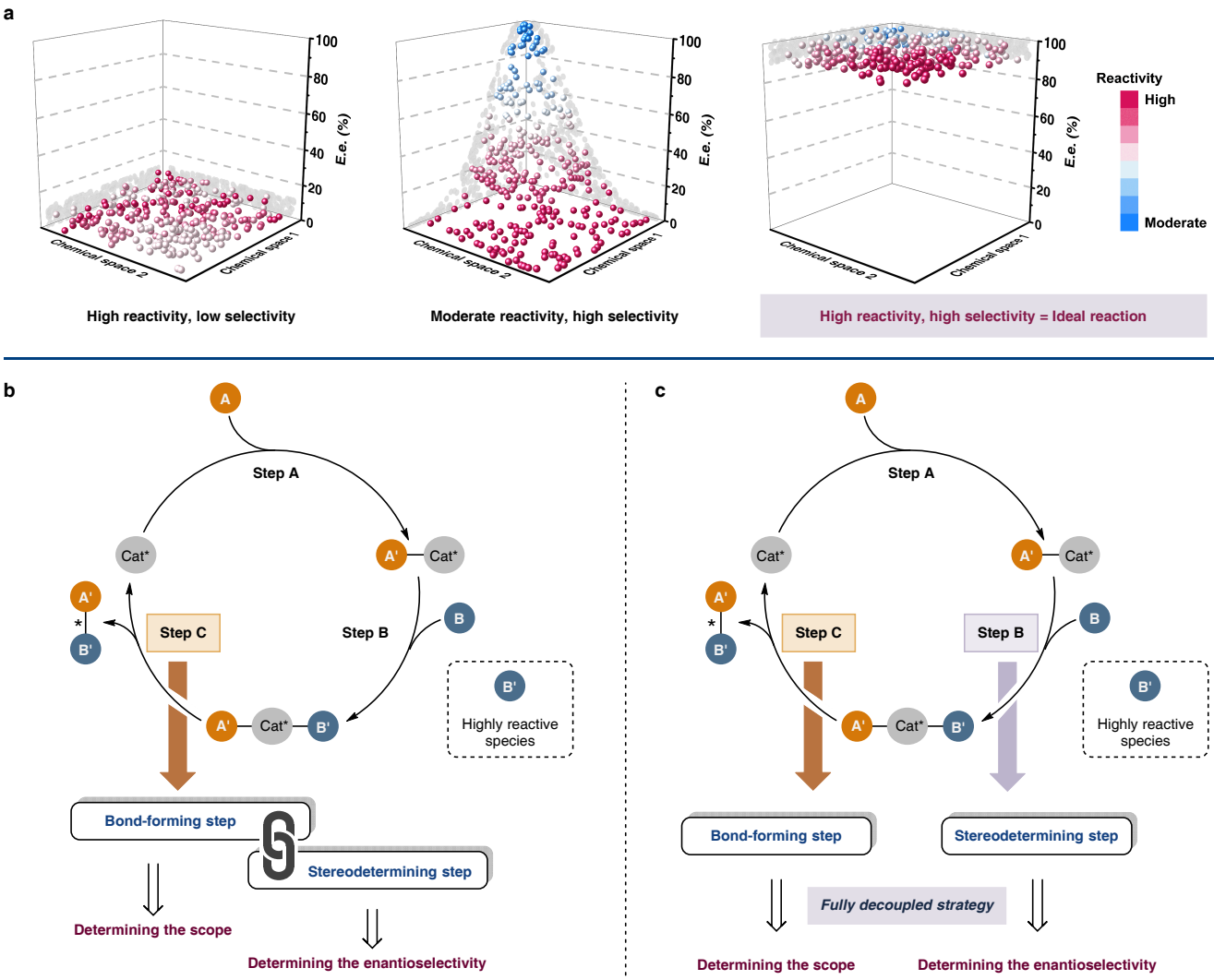

**Fig. 1 | Decoupling strategy-enabled asymmetric radical reaction generality. a**, Highly reactive species pose a great challenge for achieving both high enantioselectivity and wide reaction generality that an ideal synthetic method should possess. **b**, The major obstacle can be well appreciated in a typical bond coupling catalytic cycle where the bond-forming step and stereodetermining step are commonly coupled together. This brings about the issue of reactivity and selectivity, which are likely reciprocally correlated to each other. **c**, Separating these two steps is believed to be beneficial to mitigate the aforementioned reactivity-selectivity dilemma. **d**, This decoupling strategy allows for a copper-catalyzed general asymmetric radical cross-coupling platform, achieved by combining copper-catalyzed enantioselective S(IV) center formation with copper-sulfinimidoyl complex-mediated enantiospecific $S_H2$ radical coupling. This approach successfully accommodates an array of over 30 different radicals featuring C, N, and O centers with various levels of reactivity.

## Design plan and stoichiometric experiments

Transition metal-catalyzed asymmetric radical cross-coupling reactions have been developed rapidly in the past decade[34,35]. However, current methods heavily rely on enantioselective reductive elimination to forge stereocenters (Fig. 1b). To address the reactivity and selectivity issue through the decoupling strategy discussed above, we initially assumed that the preceding oxidative addition would determine the enantioselectivity. The following enantiospecific $S_H2$ would then deliver the enantioenriched product while maintaining a broad reaction scope. In this scenario, the stereoselective formation of a thermodynamically favored chiral L*$M^{n+1}$–Nu complex with a configurationally stable chiral nucleophile motif would be greatly preferred. With this in mind, we promptly identified sulfur nucleophiles as promising candidates given the often robust metal–S bonds[36]. In addition, S(II) and S(IV) compounds have a pronounced propensity to engage in intramolecular homolytic substitution ($S_Hi$) reactions[23,24], particularly with high

stereochemical fidelity when applicable[37]. Noteworthy is that chiral S(IV) and S(VI) centers are not only important chiral synthons in asymmetric organic synthesis but also prevalent functional groups in medicinal chemistry (Supplementary Fig. 2)[38,39]. Some elegant catalytic asymmetric methods have been disclosed for synthesizing these valuable molecules[40–42] (see Supplementary Fig. 1 for further discussions). However, a comprehensive approach to attaining assorted S(IV) and S(VI) centers with a broad spectrum of substitutions still remains to be devised.

S(IV)–metal complexes with S-stereogenic centers can be formed through S(II)/S(IV) tautomerization by bivalent sulfur compounds, such as *N*-acyl sulfenamides[43], upon deprotonation. Thus, we initially chose *N*-acyl sulfenamides as nucleophiles and started to verify the abovementioned hypothesis using several stoichiometric control experiments. With our recent achievement in copper-catalyzed asymmetric radical carbon–heteroatom bond formation[44], we reasoned that copper would be the ideal transition metal catalyst due to its high resistance to sulfur poisoning. When *N*-acyl sulfenamide **S1** was mixed with copper in the presence of base, a well-defined copper(II)–sulfinimidoyl complex **M1** was formed instead of a copper(II)–amido complex (Fig. 2a; see Supplementary Fig. 3 for its X-ray structure). More encouragingly, ethylation of the S(IV) center occurred quantitatively when **M1** was treated with triethylborane under standard conditions for ethyl radical generation. In addition to the sulfilimine product **1**, an ethylene-bonded copper(I) complex **M2** was also isolated in quantitative yield and fully characterized by X-ray diffraction analysis (Fig. 2b; see Supplementary Fig. 4 for its X-ray structure). We strongly believe that this ethylation reaction is a standard $S_H2$ process occurring on the S(IV) center, as the copper center is largely coordinately saturated. These findings suggested that copper(II) species are a viable "radical leaving group" for advancing $S_H2$-based asymmetric catalysis (e.g., Step C in Fig. 2d). Unfortunately, all attempts to isolate the optically active complex **M1** were not fruitful at this stage. To probe the stereochemistry of this $S_H2$ reaction, we investigated the intramolecular radical substitution reaction of enantioenriched

sulfilimine **2** (Fig. 2c) as a model. When treated with supersilane (tris(trimethylsilyl)silane) and triethylborane under ambient conditions, the chiral S(IV) center underwent radical substitution with 100% inversion, demonstrating high enantiospecificity. Overall, these experiments provided favorable evidence for the feasibility of a conceivable catalytic cycle involving an enantiodetermining oxidative addition followed by an enantiospecific $S_H2$ step (Fig. 2d). Thus, we proceeded to optimize the reaction conditions for catalysis, employing *N*-acyl sulfenamide **S2** and propargyl bromide **C1** as the model substrates.

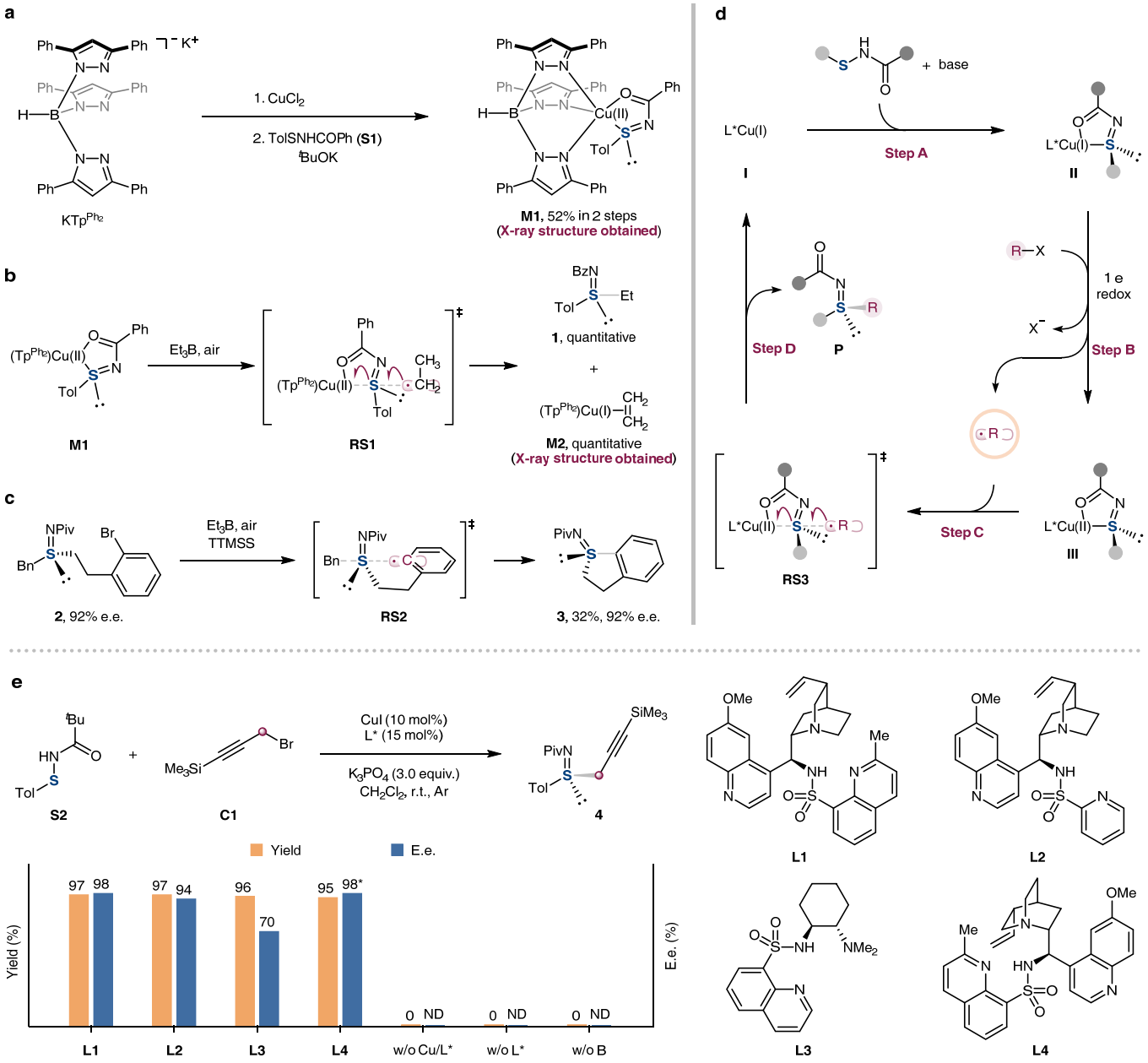


**Fig. 2 | Inspirations and reaction development. a**, Synthesis of Cu(II)-sulfinimidoyl complexes. **b**, The $S_H2$ reaction of ethyl radicals with Cu(II)–sulfinimidoyl complexes. **c**, The enantiospecific intramolecular homolytic substitution reaction of chiral sulfilimine. **d**, A proposed catalytic cycle for copper-catalyzed enantioselective radical cross-coupling of *N*-acyl sulfenamides with electrophiles via enantiospecific $S_H2$ substitution. **e**, Copper-catalyzed enantioselective S–C coupling of *N*-acyl sulfenamides with propargyl

bromides. $Tp^{Ph_2}$, hydrotris(3,5-diphenylpyrazol-1-yl)borate; Tol, *p*-tolyl; Bz, benzoyl; Bn, benzyl; Piv, pivaloyl; TTMSS, tris(trimethylsilyl)silane; w/o, without; Cu/L*, copper salt and chiral ligand; L*, chiral ligand; B, base; ND, not determined.

**Reaction development and scope**

To achieve both great reaction generality and excellent enantioselectivity, we first performed a detailed ligand screening; common commercially available neutral N- and/or P-based ligands as well as carboxamide-based anionic ligands provided moderate to good yields but only marginal enantioselectivity for the current transformation (Supplementary Table 1). By contrast, the sulfonamide-based anionic ligands **L1** to **L4** all gave both high isolated yields and excellent enantioselectivity (Fig. 2e; see Supplementary Tables 2–4 for additional condition optimization results). We speculated that these ligands might generate more configurationally stable L*Cu(II)–S(=NPiv)Tol complexes for the following $S_H2$ step.

After successfully solving the enantioselectivity issue, we proceeded to test the generality of this transformation (Fig. 3). Our first step was to investigate the electrophile scope using *N*-acyl sulfenamide **S2** as the standard nucleophile. We examined a range of alkyl halides as the precursor to alkyl radicals, which were generated using copper-catalyzed direct halogen-atom transfer (XAT) or indirect aryl radical-mediated XAT processes[45] based on literature reports. We were delighted to discover that the decoupling strategy effectively produced a diverse array of chiral sulfoximines (**4**–**6** and **10**–**25**) from various alkyl radical species (Fig. 3; see Supplementary Figs. 5 and 6 for X-ray structures of **5** and **15**, respectively) (see Supplementary Tables 5 and 6 for additional condition optimization results). These alkyl radicals exhibited varying stabilities[46], ranging from the highly stabilized benzyl radical **R7** (C–H bond-dissociation energy (BDE): 90 kcal/mol) to the very unstabilized methyl radical **R22** (C–H BDE: 105 kcal/mol), and all demonstrated excellent enantioselectivity with high isolated yields. Even the extremely reactive aryl radical

(C–H BDE: 113 kcal/mol) also delivered the arylation product **7** with 95% enantiomeric excess (e.e.) (see Supplementary Table 7 for additional condition optimization results). Besides radical stabilities, the present asymmetric cross-coupling reaction showed substantial insensitivity toward radical steric properties. This is evidenced by the fact that monosubstituted (e.g., **R1**, **R7**, **R10**, and **R17**), disubstituted (**R2**, **R13**, and **R19**), and tri-substituted alkyl radicals (e.g., **R11**, **R14**, and **R15**) all afforded good yields and excellent enantioselectivity (>90% e.e.). Perhaps most remarkably, the enantioselectivity was not affected by the radical polarity[47]. Both nucleophilic (e.g., **R10** and **R14**) and electrophilic (e.g., **R9** and **R12**) alkyl radicals exhibited comparably high enantioselectivity. More importantly, both the nucleophilic dimethylaminyl radical **R5** and the highly electrophilic *tert*-butoxyl radical **R6** smoothly underwent the coupling reaction (see Supplementary Tables 8–9 for condition optimization results), yielding chiral sulfinamidine **8** and sulfinimidate ester **9** with high e.e. It is worth to mention that the *tert*-butoxyl radical **R6** is known to undergo rapid β-scission (rate constant $k_\beta$ at 295 K in acetonitrile: $6 \times 10^4$ $s^{-1}$)[48], resulting in methyl radicals and acetone. However, in our reaction, the coupling product **9** was efficiently formed while acetone was hardly detected, indicating a very fast $S_H2$ process, as originally presumed. Interestingly, we were able to convert *N*-acyl sulfenamide **S2** to a range of chiral sulfinamidines **26**–**37** (see Supplementary Fig. **7** for the X-ray structure of **26**) using highly diverse aminyl radicals derived from their corresponding *N*-benzoyloxyamine precursors. Overall, we believe that the present transformation has an unprecedented radical scope in the field of catalytic asymmetric radical cross-coupling.

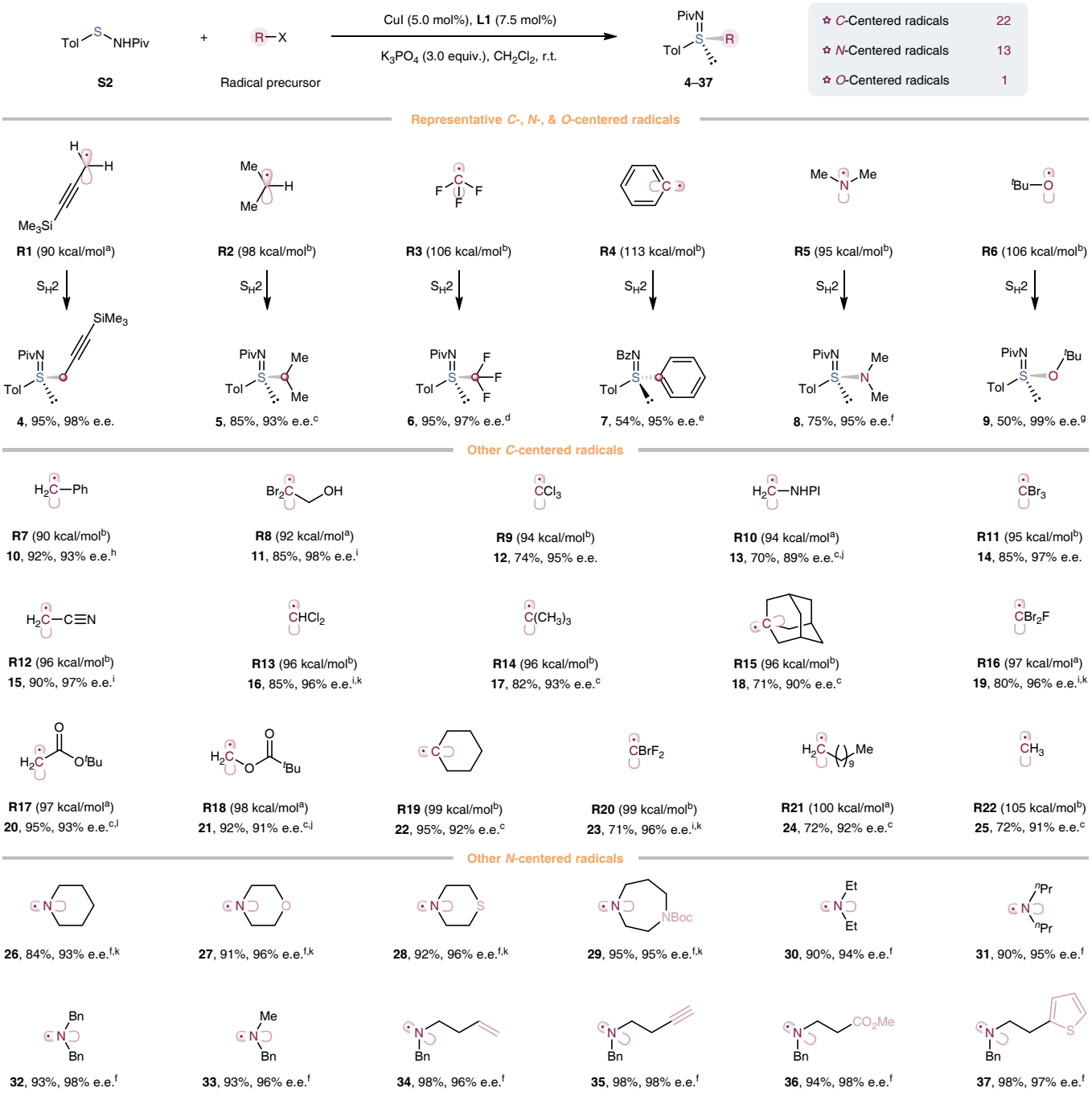


**Fig. 3 | Substrate scope of radicals.** Standard reaction conditions: *N*-acyl sulfenamide (0.20 mmol), alkyl bromide (1.2 equiv.), CuI (5.0 mol%), **L1** (7.5 mol%), and $K_3PO_4$ (3.0 equiv.) in dichloromethane (2.0 mL) at room temperature (r.t.) under argon. The yield is isolated. The e.e. values are based on chiral high-performance liquid chromatography analysis. [a]Predicted C–H BDE by DeepSynthesis at

http://pka.luoszgroup.com/bde_prediction. [b]Experimental C–H BDE from literature[46]. [c]Alkyl iodide (1.5 equiv.), CuI (10 mol%), **L3** (15 mol%), and $MesN_2BF_4$ (2.0 equiv.) in MTBE (4.0 mL). [d]Togni's reagent II (1.5 equiv.) at –10 °C. [e]$PhN_2BF_4$ (1.5 equiv.), CuI (30 mol%), and **L4** (45 mol%) in PhF (2.0 mL). [f]*N*-Benzoyloxyamine (1.5 equiv.) in EtOAc (2.0 mL). [g]$^t$BuOOH (1.2 equiv.) in $CH_3CN$ (2.0 mL) at –10 °C. In addition to **9**, the other product (*S*s)-TolS(=O)NHPiv (**9′**, 40% yield, 91% e.e.) was formed. Modifying the work-up procedure led to only **9′** in 95% yield with 96% ee (see Supplementary Fig. 11 for details). [h]**L2** (7.5 mol%). [i]Alkyl bromide (1.5 equiv.). [j]At 10 °C. [k]At 40 °C. [l]At –30 °C. BDE, bond-dissociation energy; Mes, mesityl; MTBE, methyl *tert*-butyl ether; Boc, *tert*-butyloxycarbonyl.

We next sought to evaluate the scope of the *N*-acyl sulfenamide coupling partner. As shown in Fig. 4, multiple *N*-acyl sulfenamides that contain *S*-(hetero)aryl groups having distinct electronic properties or substitution patterns produced the desired sulfilimine products (**38**–**46**) in good yields with excellent enantioselectivity. We were pleased to discover that *S*-alkyl *N*-acyl sulfenamides are suitable substrates (**47**–**57**) and that their steric properties (**54**–**56**) or preexisting stereocenters (**57**) did not impact the reaction's efficiency or enantioselectivity. Our protocols were also effective in accessing the chiral sulfinamidines (**58**–**64**) and sulfinamides (**65**–**68**)[49] with different nitrogen or oxygen electrophiles. More importantly, many medicinally important functional groups were well-tolerated, such as acetanilide (**41**), pyridine (**61**), thiophene (**46**, **62**, and **67**), furan (**63**), primary alkyl chloride (**50**), and protected galactopyranose (**57**).

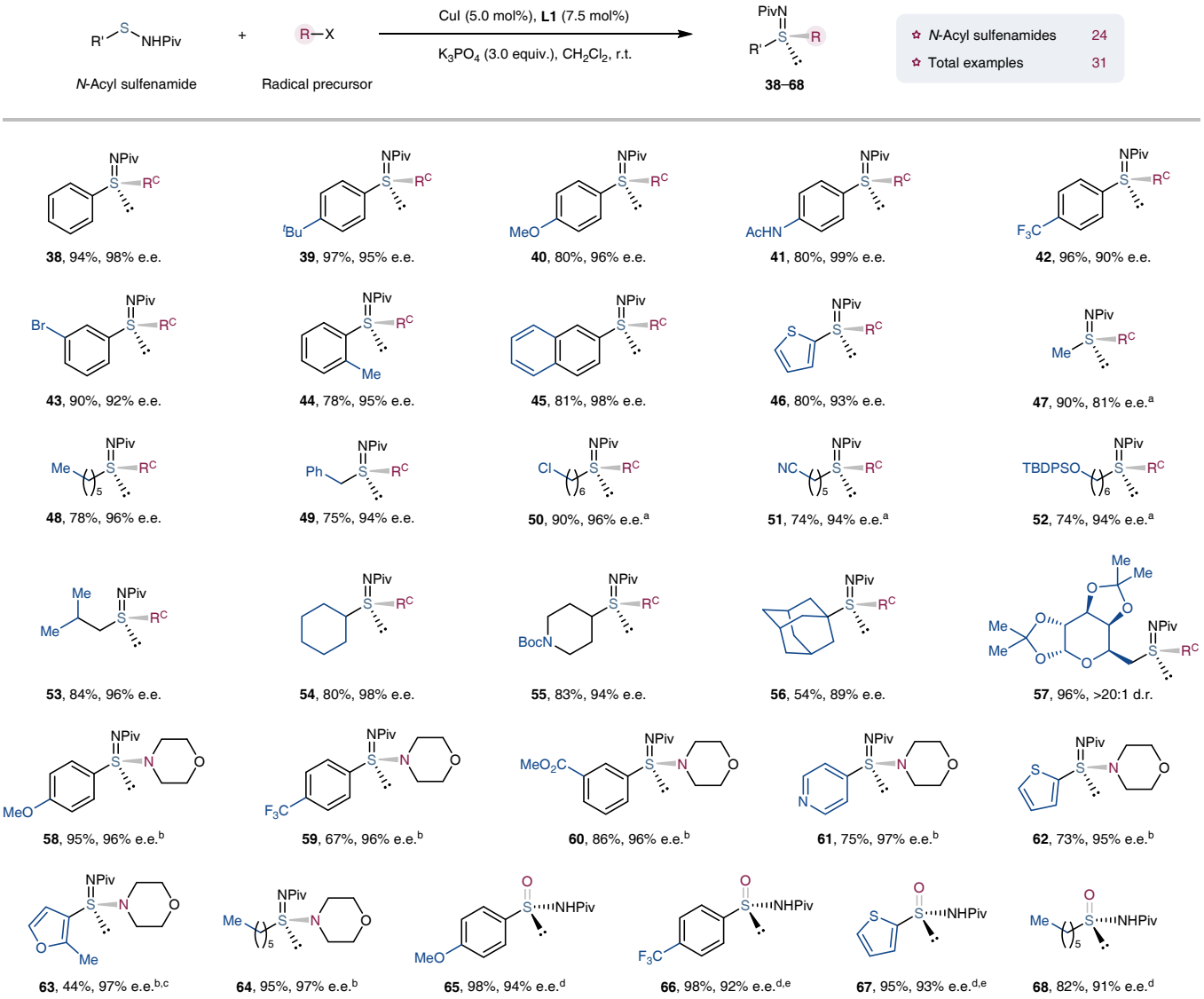


**Fig. 4 | Substrate scope of *N*-acyl sulfenamides.** Standard reaction conditions: *N*-acyl sulfenamide (0.20 mmol), alkyl bromide (1.2 equiv.), CuI (5.0 mol%), **L1** (7.5 mol%), and $K_3PO_4$ (3.0 equiv.) in dichloromethane (2.0 mL) at r.t. under argon. The yield is isolated. The e.e. values are based on chiral high-performance liquid chromatography analysis. The diastereomeric ratio (d.r.) value is based on crude $^1$H NMR analysis. [a]Alkyl bromide (1.5 equiv.). [b]*N*-Benzoyloxyamine (1.5 equiv.) in EtOAc (2.0 mL) at 40 °C. [c]At r.t. [d]$^t$BuOOH (1.2 equiv.) in $CH_3CN$ (2.0 mL) at –10 °C. [e]CuI (10 mol%) and **L1** (15 mol%) at –20 °C. $R^C$, $CH_2C{\equiv}CSiMe_3$; Ac, acetyl; TBDPS, *tert*-butyldiphenylsilyl.

## Synthetic utility

The method presented above provides a general coupling approach for converting *N*-acyl sulfenamides to a range of chiral S(IV) centers, encompassing sulfilimines, sulfinamidines, sulfinamides, and sulfinimidate esters. In addition, sulfilimine **69** (see Supplementary Fig. 16 for its synthesis) could be converted in a straightforward manner to sulfoxide **70** (Fig. 5a; see Supplementary Fig. 16 for additional examples **71** and **72**), which bear similar *S*-substituents that are otherwise challenging to differentiate stereochemically by direct oxidation methods (Supplementary Fig. 1). An intriguing prospect involves utilizing stereoselective reactions to convert these chiral S(IV) centers to their corresponding chiral S(VI) centers (Fig. 5a). As such, chiral sulfilimine **5** and sulfinamidine **26** were successfully transformed into sulfondiimine **74**, sulfoximine **75**, sulfondiimidamide **76**, and sulfonimidamide **77**, respectively, by treatment with appropriate oxidants under catalytic conditions[38]. Furthermore, sulfinamide **9′** was either alkylated to produce sulfinimidate ester **73** or oxidized to generate sulfonimidoyl fluoride **78** and sulfonimidamide **79**. Both **73**[50] and **78**[51] are well-known synthetic hubs towards a number of chiral S(IV) and S(VI) compounds. Notably, all these reactions transferred the chiral information of the S(IV) centers quantitatively to the products of S(IV) or S(VI) centers. Thus, this asymmetric radical coupling reaction offers a comprehensive synthetic solution for medicinal chemists to investigate novel chiral chemical space regarding sulfur-based bioactive molecules.

## Mechanistic study

The control experiments with radical inhibitors TEMPO ((2,2,6,6-tetramethylpiperidin-1-yl)oxyl) or BHT (butylated hydroxytoluene) all revealed substantial retardation of the coupling reactions with C-, N-, and O-based electrophiles (Supplementary Figs. 8 and 9), supporting the presumed involvement of radical species. More intriguingly, the catalytic system could convert radicals **R7** and **R12**—generated by hydrogen atom abstraction from the corresponding hydrocarbon solvents (Supplementary Fig. 10)—into the desired coupling products **10** and **15**, respectively, with high enantioselectivity, albeit in low yields. These results

further confirmed the intermediacy of radical species in the coupling reactions. To rule out a nucleophilic substitution pathway, both enantioenriched and racemic alkyl iodide **C22** were subjected to the coupling reaction conditions (Fig. 5b). The resulting product **80** displayed identical diastereoselectivity originating from the carbon stereocenters (see Supplementary Fig. 12 for details), which are in accord with the proposed radical mechanism rather than an ionic one. In addition, the control experiments in the absence of catalyst or base all failed to afford the enantioenriched products (Fig. 2e and Supplementary Tables 10 and 11), indicating both reaction components are indispensable for this transformation. Further experiments in the presence of scalemic ligands revealed a linear relationship between the enantiopurities of the ligands and their corresponding products (Supplementary Fig. 13), supporting a 1:1 ligand-to-copper ratio in the enantiodetermining step. More importantly, our initial stoichiometric experiments clearly demonstrated the ready formation of Cu(II)–sulfinimidoyl complexes and their susceptibility toward $S_H2$ substitution reactions (Fig. 2).

To further elucidate the stereospecific $S_H2$ mechanism, we performed DFT (density functional theory) calculations on the key C–S bond formation pathway (Fig. 5c, Supplementary Figs. 14 and 15, and Table 12). The Cu(II) intermediate **INT-1** and cyanomethyl radical **INT-2** undergo a C–S bond formation via an open-shell singlet transition state **TS-3**, generating **INT-4** with the formed C–S bond, which eventually liberates the observed major product **15** (Fig. 5c). For the minor product formation pathway, **INT-1** undergoes a configurational shift via **TS-5**, affording **INT-6** with the opposite chirality of sulfur. Subsequential C–S bond formation via **TS-7** generates **INT-8**, which eventually liberates the minor product (Fig. 5c). The configurational shift transitional state **TS-5** is 1.7 kcal/mol unfavorable than the $S_H2$ transition state **TS-3**. This energy difference indicates that the C–S bond formation has a lower free energy barrier and the configuration flip is unlikely. Furthermore, NBO (natural bond orbital) analysis on the C–S bond formation transition state confirms the interaction between the SOMO (singly occupied molecular

orbital) of the cyanomethyl radical and the anti-bonding orbital of the Cu–S bond in **TS-3** (Fig. 5d), which agrees with the nature of $S_H2$[22]. Based on this discussion, we propose that the C–S bond is formed via a stereospecific $S_H2$ mechanism.

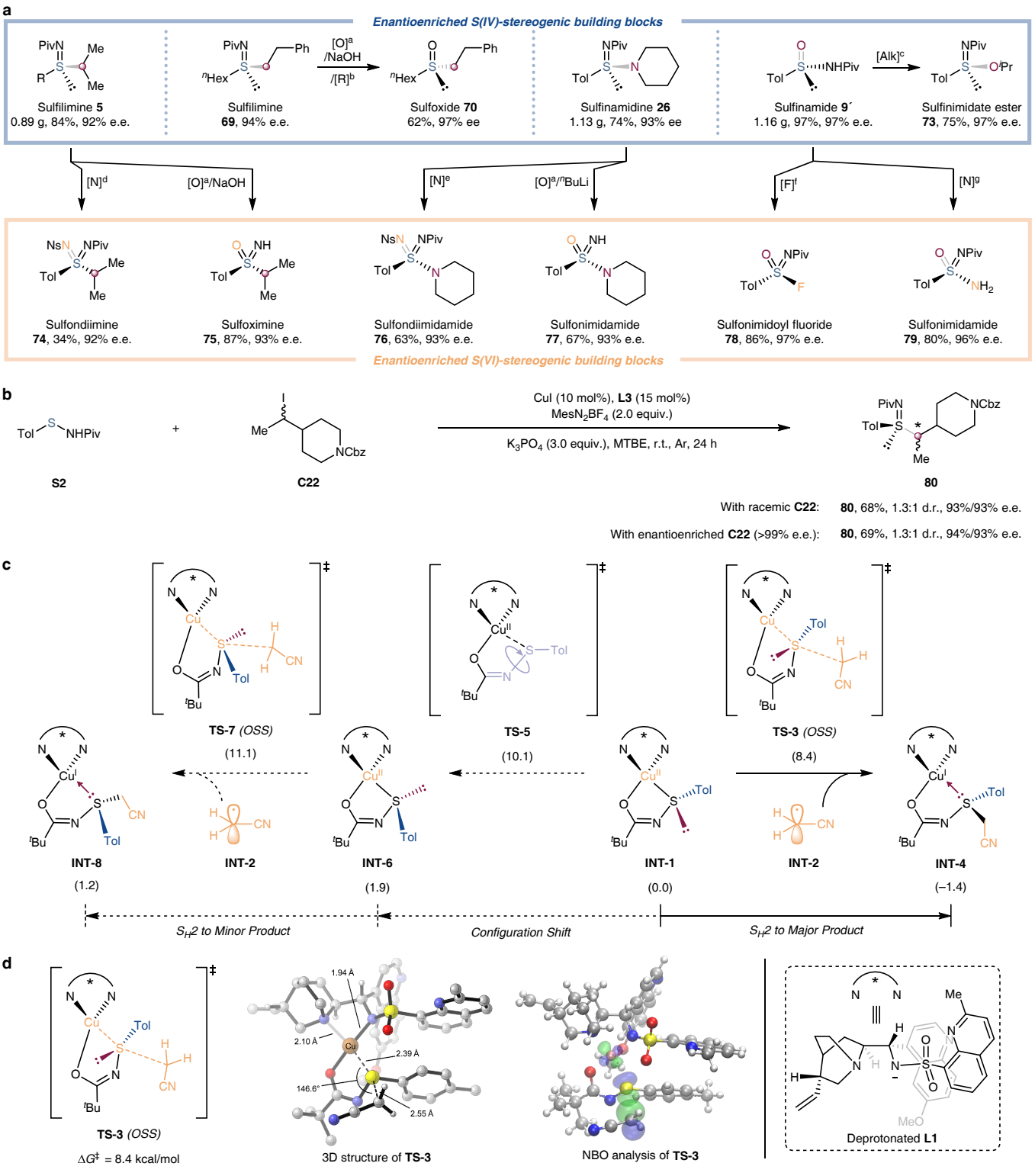


**Fig. 5 | Synthetic utility and mechanistic studies. a**, Product transformations to a variety of important chiral compounds containing S(IV) and S(VI) stereocenters. **b**, The control experiments using

enantioenriched and racemic secondary alkyl iodide substrates revealed identical diastereoselectivity, supporting the proposed radical mechanism. **c**, DFT-calculated structures and free energies (given in parentheses in kcal/mol) concerning the key C–S bond formation at the B3LYP-D3(BJ)/Def2-TZVP-SMD(Dichloromethane)//B3LYP-D3(BJ)/Def2-SVP-SMD(Dichloromethane) level of theory. **d**, The calculated structure and NBO analysis of the key C–S bond formation transition state **TS-3**. [a]$RuCl_3$ and $NaIO_4$. [b]$^t$BuONO and DTBP. [c]$^i$PrI and $K_2CO_3$. [d]AgNTf, $^t$Bu$_3$tpy, and PhI=NNs. [e]AgNTf, $^t$Bu$_3$tpy, PhI=NNs, and $NaHCO_3$. [f]NaH; Selectfluor, and KOAc. [g]$NH_3$ (aq.) and $^t$BuOCl. [O], oxidation; [R], reduction; [Alk], alkylation; [N], imidation or amination; [F], fluorination; $^n$Hex, *n*-hexyl; DTBP, 2,6-di-*tert*-butylpyridine; Tf, trifluoromethanesulfonyl; $^t$Bu$_3$tpy, 4,4',4''-tri-*tert*-butyl-2,2':6',2''-terpyridine; Ns, *p*-nitrobenzenesulfonyl; aq., aqueous solution; DFT, density functional theory; NBO, natural bond orbital.

## Summary

In summary, we have developed a highly enantioselective radical cross-coupling reaction with great generality by exploiting a decoupling strategy via enantiospecific $S_H2$ processes. The S(II) centers of *N*-acyl sulfenamides were conveniently upgraded to a variety of chiral S(IV) centers with a highly diverse range of organic radicals. The broad reaction scope and high enantioselectivity relied on the decoupling of bond-forming and stereodetermining steps. We believe that this asymmetric radical coupling strategy would be readily extended to other heteroatom-chiral centers, including phosphorous(III) and silicon(IV), and eventually achieve broad generality on chiral carbon stereocenters.

**Online content**

Any methods, additional references, Nature Research reporting summaries, source data, extended data, supplementary information, acknowledgements, peer review information; details of author contributions and competing interests; and statements of data and code availability are available at https://doi.org/10.1038/XXXXXXXXXX.

**References and Notes:**


1. Smit, W. A., Bochkov, A. F. & Caple, R. *Organic Synthesis: The Science behind the Art* (The Royal Society of Chemistry, 1998).
2. Seebach, D. Organic synthesis—where now? *Angew. Chem. Int. Ed. Engl.* **29**, 1320–1367 (1990).
3. Kürti, L. & Czakó, B. *Strategic Applications of Named Reactions in Organic Synthesis: Background and Detailed Mechanisms* (Elsevier Academic Press, 2005).
4. Collins, K. D. & Glorius, F. A robustness screen for the rapid assessment of chemical reactions. *Nat. Chem.* **5**, 597–601 (2013).
5. Blakemore, D. C. et al. Organic synthesis provides opportunities to transform drug discovery. *Nat. Chem.* **10**, 383–394 (2018).
6. Johansson Seechurn, C. C. C., Kitching, M. O., Colacot, T. J. & Snieckus, V. Palladium-catalyzed cross-coupling: A historical contextual perspective to the 2010 Nobel prize. *Angew. Chem. Int. Ed.* **51**, 5062–5085 (2012).
7. Taylor, R. D., MacCoss, M. & Lawson, A. D. G. Rings in drugs. *J. Med. Chem.* **57**, 5845–5859 (2014).

8. Farhang, M., Akbarzadeh, A. R., Rabbani, M. & Ghadiri, A. M. A retrospective-prospective review of Suzuki–Miyaura reaction: From cross-coupling reaction to pharmaceutical industry applications. *Polyhedron* **227**, 116124 (2022).

9. Strassfeld, D. A., Algera, R. F., Wickens, Z. K. & Jacobsen, E. N. A case study in catalyst generality: Simultaneous, highly-enantioselective Brønsted- and Lewis-acid mechanisms in hydrogen-bond-donor catalyzed oxetane openings. *J. Am. Chem. Soc.* **143**, 9585–9594 (2021).

10. Wagen, C. C., McMinn, S. E., Kwan, E. E. & Jacobsen, E. N. Screening for generality in asymmetric catalysis. *Nature* **610**, 680–686 (2022).

11. Rein, J. et al. Generality-oriented optimization of enantioselective aminoxyl radical catalysis. *Science* **380**, 706–712 (2023).

12. Nagib, D. A. Asymmetric catalysis in radical chemistry. *Chem. Rev.* **122**, 15989–15992 (2022).

13. Naredla, R. R. & Klumpp, D. A. Contemporary carbocation chemistry: Applications in organic synthesis. *Chem. Rev.* **113**, 6905–6948 (2013).

14. Albarrán-Velo, J., González-Martínez, D. & Gotor-Fernández, V. Stereoselective biocatalysis: A mature technology for the asymmetric synthesis of pharmaceutical building blocks. *Biocatal. Biotransform.* **36**, 102–130 (2018).

15. Emmanuel, M. A. et al. Photobiocatalytic strategies for organic synthesis. *Chem. Rev.* **123**, 5459–5520 (2023).

16. Dong, X.-Y. et al. A general asymmetric copper-catalysed Sonogashira C($sp^3$)–C($sp$) coupling. *Nat. Chem.* **11**, 1158–1166 (2019).

17. Kim, H. et al. A multi-substrate screening approach for the identification of a broadly applicable Diels–Alder catalyst. *Nat. Commun.* **10**, 770 (2019).

18. Proctor, R. S. J., Colgan, A. C. & Phipps, R. J. Exploiting attractive non-covalent interactions for the enantioselective catalysis of reactions involving radical intermediates. *Nat. Chem.* **12**, 990–1004 (2020).

19. Chen, G. et al. Ligand-accelerated enantioselective methylene C($sp^3$)–H bond activation. *Science* **353**, 1023–1027 (2016).

20. Cheng, Q. et al. Iridium-catalyzed asymmetric allylic substitution reactions. *Chem. Rev.* **119**, 1855–1969 (2019).

21. Newton, C. G., Wang, S.-G., Oliveira, C. C. & Cramer, N. Catalytic enantioselective transformations involving C–H bond cleavage by transition-metal complexes. *Chem. Rev.* **117**, 8908–8976 (2017).

22. Walton, J. C. Homolytic substitution: A molecular ménage à trois. *Acc. Chem. Res.* **31**, 99–107 (1998).

23. Crich, D. Homolytic substitution at the sulfur atom as a tool for organic synthesis. *Helv. Chim. Acta* **89**, 2167–2182 (2006).

24. Garrido-Castro, A. F., Salaverri, N., Maestro, M. C. & Alemán, J. Intramolecular homolytic substitution enabled by photoredox catalysis: Sulfur, phosphorus, and silicon heterocycle synthesis from aryl halides. *Org. Lett.* **21**, 5295–5300 (2019).

25. Liu, W., Lavagnino, M. N., Gould, C. A., Alcázar, J. & MacMillan, D. W. C. A biomimetic $S_H2$ cross-coupling mechanism for quaternary $sp^3$-carbon formation. *Science* **374**, 1258–1263 (2021).

26. Meunier, B., de Visser, S. P. & Shaik, S. Mechanism of oxidation reactions catalyzed by cytochrome P450 enzymes. *Chem. Rev.* **104**, 3947–3980 (2004).

27. Tian, Y. et al. A general copper-catalysed enantioconvergent C($sp^3$)–S cross-coupling via biomimetic radical homolytic substitution. *Nat. Chem.*, DOI: 10.1038/s41557-023-01385-w (2023).

28. Cheng, Y.-F. et al. Cu-catalysed enantioselective radical heteroatomic S–O cross-coupling. *Nat. Chem.* **15**, 395–404 (2023).

29. Gould, C. A., Pace, A. L. & MacMillan, D. W. C. Rapid and modular access to quaternary carbons from tertiary alcohols via bimolecular homolytic substitution. *J. Am. Chem. Soc.* **145**, 16330–16336 (2023).

30. Zhang, R. K. et al. Enzymatic assembly of carbon–carbon bonds via iron-catalysed $sp^3$ C–H functionalization. *Nature* **565**, 67–72 (2019).

31. Lee, W.-C. C., Wang, D.-S., Zhu, Y. & Zhang, X. P. Iron(III)-based metalloradical catalysis for asymmetric cyclopropanation via a stepwise radical mechanism. *Nat. Chem.* **15**, 1569–1580 (2023).

32. Milan, M., Bietti, M. & Costas, M. Enantioselective aliphatic C–H bond oxidation catalyzed by bioinspired complexes. *Chem. Commun.* **54**, 9559–9570 (2018).

33. Upton, C. J. & Incremona, J. H. Bimolecular homolytic substitution at carbon. A stereochemical investigation. *J. Org. Chem.* **41**, 523–530 (1976).

34. Cherney, A. H., Kadunce, N. T. & Reisman, S. E. Enantioselective and enantiospecific transition-metal-catalyzed cross-coupling reactions of organometallic reagents to construct C–C bonds. *Chem. Rev.* **115**, 9587–9652 (2015).

35. Choi, J. & Fu, G. C. Transition metal–catalyzed alkyl-alkyl bond formation: Another dimension in cross-coupling chemistry. *Science* **356**, eaaf7230 (2017).

36. Omann, L., Königs, C. D. F., Klare, H. F. T. & Oestreich, M. Cooperative catalysis at metal–sulfur bonds. *Acc. Chem. Res.* **50**, 1258–1269 (2017).

37. Coulomb, J. et al. Intramolecular homolytic substitution of sulfinates and sulfinamides. *Chem. Eur. J.* **15**, 10225–10232 (2009).

38. Zhang, X., Wang, F. & Tan, C.-H. Asymmetric synthesis of S(IV) and S(VI) stereogenic centers. *JACS Au* **3**, 700–714 (2023).

39. Zhang, Z.-X. & Willis, M. C. Sulfondiimidamides as new functional groups for synthetic and medicinal chemistry. *Chem* **8**, 1137–1146 (2022).

40. Zhang, X., Ang, E. C. X., Yang, Z., Kee, C. W. & Tan, C.-H. Synthesis of chiral sulfinate esters by asymmetric condensation. *Nature* **604**, 298–303 (2022).

41. Greenwood, N. S., Champlin, A. T. & Ellman, J. A. Catalytic enantioselective sulfur alkylation of sulfenamides for the asymmetric synthesis of sulfoximines. *J. Am. Chem. Soc.* **144**, 17808–17814 (2022).

42. van Dijk, L. et al. Data science-enabled palladium-catalyzed enantioselective aryl-carbonylation of sulfonimidamides. *J. Am. Chem. Soc.* **145**, 20959–20967 (2023).

43. Zhong, W. et al. Synthesis and reactivity of the imido-bridged metallothiocarboranes $CpCo(S_2C_2B_{10}H_{10})(NSO_2R)$. *Organometallics* **31**, 6658–6668 (2012).

44. Chen, J.-J. et al. Enantioconvergent Cu-catalysed *N*-alkylation of aliphatic amines. *Nature* **618**, 294–300 (2023).

45. Cai, A., Yan, W., Wang, C. & Liu, W. Copper-catalyzed difluoromethylation of alkyl iodides enabled by aryl radical activation of carbon–iodine bonds. *Angew. Chem. Int. Ed.* **60**, 27070–27077 (2021).

46. Luo, Y.-R. *Comprehensive Handbook of Chemcial Bond Energies* (CRC Press, 2007).

47. Parsaee, F. et al. Radical philicity and its role in selective organic transformations. *Nat. Rev. Chem.* **5**, 486–499 (2021).

48. Tsentalovich, Y. P., Kulik, L. V., Gritsan, N. P. & Yurkovskaya, A. V. Solvent effect on the rate of *β*-scission of the *tert*-butoxyl radical. *J. Phys. Chem. A* **102**, 7975–7980 (1998).

49. Robak, M. T., Herbage, M. A. & Ellman, J. A. Synthesis and applications of *tert*-butanesulfinamide. *Chem. Rev.* **110**, 3600–3740 (2010).

50. Tsuzuki, S. & Kano, T. Asymmetric synthesis of chiral sulfimides through the *O*-alkylation of enantioenriched sulfinamides and addition of carbon nucleophiles. *Angew. Chem. Int. Ed.* **62**, e202300637 (2023).

51. Homer, J. A. et al. Sulfur fluoride exchange. *Nat. Rev. Methods Primers* **3**, 58 (2023).

## Methods

Descriptions of the methods used are provided in the Supplementary Information.

## Data availability

The data supporting the findings of this study are available within the paper and its Supplementary Information (experimental procedures, characterization data, and DFT calculations). Crystallographic data are also free of charge from the Cambridge Crystallographic Database Centre (CCDC) under CCDC reference numbers 2289793 (for **M1**), 2289792 (for **5**), 2289795 (for **15**), and 2289794 (for **26**).

## Acknowledgements

The authors appreciate the assistance of SUSTech Core Research Facilities. Financial support from the National Natural Science Foundation of China (Nos. 22025103, 92256301, and 21831002 to X.-Y.L.; 22001109 and 22271133 to Q.-S.G.; 22122109 and 22271253 to X.H.), the National Key R&D Program of China (Nos. 2021YFF0701604 and 2021YFF0701704 to X.-Y.L.; 2022YFC3401104 to Z.D.; 2022YFA1504301 to X.H.), Guangdong Innovative Program (No. 2019BT02Y335 to X.-Y.L.; 2021ZT09C278 to Z.D.), Shenzhen Science and Technology Program (Nos. KQTD20210811090112004 to X.-Y.L. and Q.-S.G.; JCYJ20220818100600001 to X.-Y.L.; JCYJ20220818100604009 to J.-B.T.; 20220814231741002 to Z.D.), Shenzhen Key Laboratory of Cross-Coupling Reactions (No. ZDSYS20220328104200001 to X.-Y.L. and Z.D.), New Cornerstone Science Foundation through the XPLORER PRIZE (to X.-Y.L.), Zhejiang Provincial Natural Science Foundation of China (No. LDQ23B020002 to X.H.), the Starry Night Science Fund of Zhejiang University Shanghai Institute for Advanced Study (No. SN-ZJU-SIAS-006 to X.H.), the Leading Innovation Team grant from Department of Science and Technology of Zhejiang Province (No. 2022R01005 to X.H.) is acknowledged. Computational studies are supported by Center for Computational Science and Engineering of Southern University of Science and Technology.

## Author contributions

L.-W.F., J.-B.T., and L.-L.W. designed the experiments and analyzed the data. L.-W.F., J.-B.T., L.-L.W., Z.-L.L., Y.-S.Z., D.-L.Y., L.Q., and C.L. performed the experiments. J.-R.L. and X.H. designed the DFT calculations and J.-R.L. performed the DFT calculations. Q.-S.G., X.H., Z.D., and X.-Y.L. wrote the manuscript. Q.-S.G., Z.D., and X.-Y.L. conceived and supervised the project.

## Competing interests

Authors declare no competing interests.

## Additional information

**Supplementary information** The online version contains supplementary material available at https://doi.org/10.1038/XXXXXX.

**Correspondence and requests for materials** should be addressed to Qiang-Shuai Gu, Xin Hong, Zhe Dong or Xin-Yuan Liu.